This is a preprint, the final version is subject to change, of the American Mineralogist (MSA)
Cite as Authors (Year) Title. American Mineralogist, in press.
(DOI will not work until issue is live.) DOI: http://dx.doi.org/10.2138/am-2017-6032

Revision 3

Addibischoffite, $Ca_2Al_6Al_6O_{20}$, a new calcium aluminate mineral from the Acfer 214 CH carbonaceous chondrite: A new refractory phase from the solar nebula

Chi Ma[1,*], Alexander N. Krot[2], Kazuhide Nagashima[2]

[1]Division of Geological and Planetary Sciences, California Institute of Technology, Pasadena, California 91125, USA
[2]Hawai'i Institute of Geophysics and Planetology, University of Hawai'i at Mānoa, Honolulu, Hawai'i 96822, USA

ABSTRACT

Addibischoffite (IMA 2015-006), $Ca_2Al_6Al_6O_{20}$, is a new calcium aluminate mineral that occurs with hibonite, perovskite, kushiroite, Ti-kushiroite, spinel, melilite, anorthite and FeNi-metal in the core of a Ca-Al-rich inclusion (CAI) in the Acfer 214 CH3 carbonaceous chondrite. The mean chemical composition of type addibischoffite by electron probe microanalysis is (wt%) Al_2O_3 44.63, CaO 15.36, SiO_2 14.62, V_2O_3 10.64, MgO 9.13, Ti_2O_3 4.70, FeO 0.46, total 99.55, giving rise to an empirical formula of $(Ca_{2.00})(Al_{2.55}Mg_{1.73}V^{3+}_{1.08}Ti^{3+}_{0.50}Ca_{0.09}Fe^{2+}_{0.05})_{\Sigma 6.01}(Al_{4.14}Si_{1.86})O_{20}$. The general formula is $Ca_2(Al,Mg,V,Ti)_6(Al,Si)_6O_{20}$. The end-member formula is $Ca_2Al_6Al_6O_{20}$. Addibischoffite has the $P\bar{1}$ aenigmatite structure with a = 10.367 Å, b = 10.756 Å, c = 8.895 Å, α = 106.0°, β = 96.0°, γ = 124.7°, V = 739.7 Å^3, and Z = 2, as revealed by electron back-scatter diffraction. The calculated density using the measured composition is 3.41 g/cm^3. Addibischoffite is a new member of the warkite ($Ca_2Sc_6Al_6O_{20}$) group and a new refractory phase formed in the solar nebula, most likely as a result of crystallization from an ^{16}O-rich Ca, Al-rich melt under high-temperature (~1575°C) and low-pressure (~10^{-4}–10^{-5} bar) conditions in the CAI-forming region near the protosun, providing a new puzzle piece toward

understanding the details of nebular processes. The name is in honor of Addi Bischoff, cosmochemist at University of Münster, Germany, for his many contributions to research on mineralogy of carbonaceous chondrites, including CAIs in CH chondrites.

Keywords: addibischoffite, $Ca_2Al_6Al_6O_{20}$, new mineral, warkite group, refractory phase, Ca-Al-rich inclusion, Acfer 214 meteorite, CH3 carbonaceous chondrite

---

*E-mail: chi@gps.caltech.edu

INTRODUCTION

During a mineralogical investigation of the Acfer 214 meteorite, CH3 metal-rich carbonaceous chondrite found in Algeria in 1991, a new calcium aluminate, $Ca_2Al_6Al_6O_{20}$ with the $P\bar{1}$ aenigmatite structure, named "addibischoffite", was identified in a Ca-Al-rich inclusion (CAI) 1580-1-8 (Fig. 1). To characterize its chemical and oxygen-isotope compositions, structure, and associated phases, we used high-resolution scanning electron microscopy (SEM), electron back-scatter diffraction (EBSD), electron probe microanalysis (EPMA) and secondary ion mass-spectrometry (SIMS). Synthetic $CaAl_6O_{10}$ was reported but not fully characterized (e.g., Inoue and Ikeda 1982; Balakaeva and Aldabergenov 2012). We describe here the first occurrence of $Ca_2Al_6Al_6O_{20}$ in a primitive meteorite, as a new refractory mineral, and discuss its origin and significance for nebular processes. Preliminary results of this work were given by Ma et al. (2016a).

MINERAL NAME AND TYPE MATERIAL

The new mineral and its name have been approved by the Commission on New Minerals, Nomenclature and Classification of the International Mineralogical Association (IMA 2015-006) (Ma and Krot 2015). The mineral name is in honor of Addi Bischoff (born in 1955), cosmochemist at University of Münster, Germany, for his many contributions to research on mineralogy of carbonaceous chondrites, including CAIs from CH chondrites. The type specimen is in section Acfer 214-1580 in G. J. Wasserburg's Meteorite Collection of Division of Geological and Planetary Sciences, California Institute of Technology, Pasadena, California 91125, USA.

APPEARANCE, OCCURRENCE AND ASSOCIATED MINERALS

Addibischoffite occurs as one irregular crystal, 9 μm × 3.5 μm in size, which is the holotype material, with hibonite, perovskite, kushiroite, Ti-kushiroite, spinel, melilite, anorthite, and FeNi-metal ($Fe_{95}Ni_5$) in the core of the Acfer 214 CAI, surrounded by a Ti-poor Al-diopside rim enclosing and intergrown with small grains of low-Ca pyroxene (Fig. 1). The CAI is ~50 μm in diameter in section Acfer 214-1580.

Addibischoffite is present in the center of the CAI where it is overgrown by kushiroite and Ti-kushiroite, and poikilitically encloses euhedral elongated crystals of hibonite and spinel, which are often intergrown. Melilite is a minor phase that is heavily corroded by anorthite that forms a compact groundmass of the CAI. The abundance of hibonite and spinel grains and their sizes decrease towards the peripheral portion of the inclusion. The Al-diopside rim has a polycrystalline compact appearance. Modal mineral abundances calculated using backscatter electron image of the CAI (surface area %) are anorthite (46), hibonite+spinel (23), kushiroite+Ti-kushiroite (6), addibischoffite (3), melilite (1), Al-diopside (20), low-Ca pyroxene (2), Fe,Ni-metal (trace) and perovskite (trace).

CHEMICAL AND OXYGEN ISOTOPIC COMPOSITIONS

Backscatter electron (BSE) images were obtained using a ZEISS 1550VP field emission SEM and a JEOL 8200 electron microprobe with solid-state BSE detectors. Six quantitative elemental microanalyses of type addibischoffite were carried out using the JEOL 8200 electron microprobe operated at 10 kV (for smaller interaction volume) and 5 nA in focused beam mode. Analyses were processed with the CITZAF correction procedure (Armstrong 1995) using the Probe for EPMA program from Probe Software, Inc. Analytical results are given in Table 1. The empirical formula (based on 20 oxygen atoms *pfu*) of type addibischoffite is $(Ca_{2.00})(Al_{2.55}Mg_{1.73}V^{3+}_{1.08}Ti^{3+}_{0.50}Ca_{0.09}Fe^{2+}_{0.05})_{\Sigma 6.01}(Al_{4.14}Si_{1.86})O_{20}$. The general formula is $Ca_2(Al,Mg,V,Ti)_6(Al,Si)_6O_{20}$, containing a minor rhönite [$Ca_2(Mg_4FeTi)(Si_3Al_3)O_{20}$] component. The end-member formula is $Ca_2Al_6Al_6O_{20}$, which requires Al_2O_3 84.51, CaO 15.49, total 100.00 wt%. The kushiroite grain in contact with type addibischoffite has an empirical formula of $Ca_{1.01}(Al_{0.66}Mg_{0.21}Ti^{4+}_{0.11}Fe_{0.02}V^{3+}_{0.02})(Si_{1.17}Al_{0.83})O_6$, whereas the nearby Ti-rich kushiroite shows an empirical formula of $(Ca_{0.97}Mg_{0.03})(Al_{0.35}Ti^{3+}_{0.28}Mg_{0.21}Ti^{4+}_{0.12}V_{0.04})(Si_{1.02}Al_{0.98})O_6$ with

a minor grossmanite component. The name kushiroite is assigned to the clinopyroxene using the valence-dominant rule for grossmanite, davisite and kushiroite (Ma et al. 2010).

Oxygen isotopic compositions of addibischoffite, hibonite, and Al-diopside were measured *in situ* with the University of Hawai'i CAMECA ims-1280 SIMS using a primary Cs^+ ion beam accelerated to 10 keV and impacted the sample with an energy of 20 keV. A Cs^+ primary beam of ~20 pA focused to ~ 1–2 μm was used for pre-sputtering (180 s) and data collection (30 cycles of 20 s each). $^{16}O^-$, $^{17}O^-$, and $^{18}O^-$ were measured simultaneously using multicollection Faraday cup (FC), monocollection electron multiplier (EM), and multicollection EM, respectively. The mass resolving power on $^{16}O^-$ and $^{18}O^-$ was ~2000, while $^{17}O^-$ was measured with a mass resolving power of ~5500, sufficient to separate interfering $^{16}OH^-$. A normal incident electron flood gun was used for charge compensation. Data were corrected for FC background, EM deadtime, tail correction of $^{16}OH^-$, and instrumental mass fractionation (IMF). Because of the abundance sensitivity tail on the OH^- peak, we made a small tail correction (typically ~ 0.2–0.5‰) on $^{17}O^-$ based on $^{16}OH^-$ count rate measured after each measurement. The IMF effects were corrected by standard-sample bracketing; for addibischoffite and hibonite using the Burma spinel standard; for high-Ca pyroxene using the Cr-augite standard. The reported 2σ uncertainties include both the internal measurement precision on an individual analysis and the external reproducibility for standard measurements. The external reproducibility of standard measurements (2 standard deviations) for both $\delta^{17}O$ and $\delta^{18}O$ was ~ ±2‰. Oxygen-isotope compositions, summarized in Table 2, are reported as $\delta^{17}O$ and $\delta^{18}O$, deviations from Standard Mean Ocean Water (SMOW) in parts per thousand:

$\delta^{17,18}O_{SMOW} = [(^{17,18}O/^{16}O_{sample})/(^{17,18}O/^{16}O_{SMOW}) - 1] \times 1000$, and as $\Delta^{17}O$ ($= \delta^{17}O - 0.52\times\delta^{18}O$), deviation from the terrestrial fractionation (TF) line.

Addibischoffite and hibonite have similar ^{16}O-rich compositions ($\Delta^{17}O = -24\pm2$‰); the Al-diopside rim is ^{16}O-depleted ($\Delta^{17}O = -6\pm3$‰; Table 2). On a three-isotope oxygen diagram (Fig. 3), compositions of addibischoffite and hibonite are displaced to the right from the Carbonaceous Chondrite Anhydrous Mineral (CCAM) line. This may be due either to melt evaporation prior or during CAI crystallization or as a result of using a poorly matched standard (Burma spinel) for IMF corrections.

CRYSTALLOGRAPHY

Single-crystal electron backscatter diffraction (EBSD) analyses at a sub-micrometer scale were performed using an HKL EBSD system on a ZEISS 1550VP SEM, operated at 20 kV and 6 nA in focused beam mode with a 70° tilted stage and in a variable pressure mode (25 Pa) (Ma and Rossman 2008, 2009). The EBSD system was calibrated using a single-crystal silicon standard. The structure was determined and cell constants were obtained by matching the experimental EBSD patterns with structures of aenigmatite, rhönite, serendibite, krinovite, and makarochkinite.

The EBSD patterns match the $P\bar{1}$ aenigmatite structure and give a best fit using the Allende rhönite structure from Bonaccorsi et al. (1990) (Fig. 2), with a mean angular deviation of 0.28º to 0.33º, showing a = 10.367 Å, b = 10.756 Å, c = 8.895 Å, α = 106.0°, β = 96.0°, γ = 124.7°, V = 739.7 Å^3, and Z = 2. The calculated density is 3.41 g/cm^3 using the empirical formula. Calculated X-ray powder diffraction data are given in Tables S1.

ORIGIN AND SIGNIFICANCE

Addibischoffite, $Ca_2Al_6Al_6O_{20}$, is a new member of the warkite group in the sapphirine supergroup. It is the Al-analog of warkite $CaSc_6Al_6O_{20}$ (Ma et al. 2015), or beckettite $Ca_2V_6Al_6O_{20}$ (Ma et al. 2016b). Addibischoffite is a new refractory phase with a minor rhönite component, and like warkite and rhönite, it is a primary phase, and, therefore, among the first solid materials formed in the solar nebula, whereas beckettite is a secondary phase formed during metasomatic alteration on the CV (Vigarano type) carbonaceous chondrite parent asteroid.

The rounded shape and compact texture of the CAI suggest its crystallization from a melt. Textural relationships between the CAI minerals imply the following crystallization sequence: hibonite + spinel → addibischoffite + melilite + kushiroite + Ti-kushiroite → anorthite → Al-diopside + low-Ca pyroxene. The ^{16}O-rich compositions of hibonite and addibischoffite indicate that these minerals crystallized a refractory ^{16}O-rich melt with Δ^{17}O of –24±2‰. This value is similar to the inferred oxygen-isotope composition of the Sun (McKeegan et al. 2011) and oxygen-isotope compositions of the majority of CAIs from unmetamorphosed chondrites (e.g., Kööp et al. 2016; Krot et al. 2017a), suggesting that the precursor material was probably an aggregate of refractory solids formed by condensation and/or evaporation in a gas of approximately solar composition in the CAI-forming region. The ^{16}O-depleted composition of

the Al-diopside rim ($\Delta^{17}O$ = –6±3‰) relative to hibonite and addibischoffite, its compact igneous-like texture, chondrule-like chemical composition ($Fs_2Wo_{45–48}$, 0.7 wt% Cr_2O_3), and the presence of small inclusions of low-Ca pyroxene, all indicate an igneous origin of the rim, most likely as a result of incomplete melting during chondrule formation of chondrule-like ferromagnesian silicate dust that accreted on the surface of the host CAI (Krot et al. 2017b). Mineralogical and isotopic observations, experimental studies, and thermodynamic analysis, all indicate that chondrule formation occurred in an ^{16}O-poor gaseous reservoir, under high total and partial SiO gas pressures, and high dust/gas ratio (~100–1000× solar), required to stabilize silicate melts and prevent significant mass-dependent fractionation effects in volatile and moderately-volatile elements (e.g., Alexander et al. 2008; Alexander and Ebel 2012; Tenner et al. 2015). The nearly complete absence of melilite in the CAI and the presence of abundant anorthite could be due to gaseous SiO – melt interaction during this melting (Libourel et al. 2006; Krot et al. 2016):

$$Ca_2Al_2SiO_{7(s)} + 3SiO_{(g)} + Mg_{(g)} + 4H_2O_{(g)} = CaAl_2Si_2O_{8(s)} + CaMgSi_2O_{6(s)} + 4H_{2(g)}$$

gehlenite — anorthite — diopside

As a result of open-system behavior of the CAI melt, its bulk chemical composition of 1580-1-8 does not reflect that of its precursor. Assuming that all anorthite in this CAI resulted from SiO gas-melt interaction, its modal mineralogy can be used to calculate bulk chemical composition of the CAI precursor (in wt%): SiO_2 (16.0), TiO_2 (0.9), Al_2O_3 (50.7), FeO (0.3), MgO (1.6), CaO (29.2), and V_2O_3 (0.4). Melt of this composition has liquidus temperature of 1575±20°C and would crystallize to form hibonite (~25%), gehlenite (~70%), and anorthite (~5%). The amount of crystallizing anorthite could be higher, if not all anorthite in the CAI resulted from gas-melt interaction during chondrule formation.

We infer that addibischoffite-bearing CAI 1580-1-8 experienced at least two melting events in isotopically distinct protoplanetary disk regions – in an ^{16}O-rich solar-like gaseous reservoir, most likely in the CAI-forming region near the protosun, and in an ^{16}O-depleted reservoir, most likely in a dust-rich region during chondrule formation. This interpretation provides clear evidence for multistage thermal processing of dust in the protoplanetary disk during localized transient heating events. It is also consistent with an age difference between

CAIs and chondrules, as commonly inferred based on their ^{26}Al-^{26}Mg isotope systematics (e.g., Kita and Ushikubo 2012; Kita et al. 2013).

IMPLICATIONS

Addibischoffite is unique so far, identified only in one CAI from Acfer 214. It most likely formed by crystallization from an ^{16}O-rich Ca, Al-rich melt under high-temperature (~1575°C) and low-pressure (~10^{-4}–10^{-5} bar) conditions in the CAI-forming region near the protosun, along with melilite and kushiroite after formation of hibonite and spinel. Calcium aluminate minerals identified in the meteorites, now including hibonite ($CaAl_{12}O_{19}$), grossite ($CaAl_4O_7$), krotite ($CaAl_2O_4$) (Ma et al. 2011) and addibischoffite ($Ca_2Al_6Al_6O_{20}$), are refractory phases occurring in CAIs that formed in the solar nebula.

Addibischoffite is one of thirteen newly-found refractory minerals discovered in CAIs from carbonaceous chondrites since 2007. Studies of these earliest solid materials are invaluable for understanding the details of nebular processes (evaporation, condensation, chemical and isotopic fractionation) in the early solar system. New refractory minerals are still being discovered in primitive meteorites like Allende (Ma 2015). These refractory minerals continue providing new puzzle pieces toward revealing the big picture of nebular evolution.

ACKNOWLEDGEMENTS

SEM, EBSD and EPMA were carried out at the Geological and Planetary Science Division Analytical Facility, Caltech, which is supported in part by NSF grants EAR-0318518 and DMR-0080065. This work was also supported by NASA grant NNX15AH38G. We thank Guy Libourel for help in estimating liquidus temperature of the CAI melt. We thank Sara Russell, Jangmi Han, and associate editor Steve Simon for their constructive reviews.

REFERENCES CITED

Alexander, C.M.O'D., Grossman, J.N., Ebel, D.S., and Ciesla, F.J. (2008) The formation conditions of chondrules and chondrites. Science, 320, 1617–1619.

Alexander, C.M.O'D. and Ebel, D.S. (2012) Questions, questions: Can the contradictions between the petrologic, isotopic, thermodynamic, and astrophysical constraints on chondrule formation be resolved? Meteoritics & Planetary Science, 47, 1157–1175.

Armstrong, J.T. (1995) CITZAF: A package of correction programs for the quantitative electron beam X-ray analysis of thick polished materials, thin films, and particles. Microbeam Analysis, 4, 177–200.

Balakaeva, G.T. and Aldabergenov, M.K. (2012) The Gibbs function normalized to the total number of electrons. Journal of Materials Science and Engineering, B 2, 394–403.

Bonaccorsi, E., Merlino, S., and Pasero, M. (1990) Rhönite: structural and microstructural features, crystal chemistry and polysomatic relationships. European Journal of Mineralogy, 2, 203–218.

Inoue, K. and Ikeda, T. (1982) The solid solution state and the crystal structure of calcium ferrite formed in lime-fluxed iron ores. Iron and Steel (in Japanese), 15, 126–135.

Kita, N.T. and Ushikubo, T. (2012) Evolution of protoplanetary disk inferred from ^{26}Al chronology of individual chondrules. Meteoritics & Planetary Science, 47, 1108–1119.

Kita, N.T., Yin, Q.-Z., MacPherson, G.J., Ushikubo, T., Jacobsen, B., Nagashima, K., Kurahashi, E., Krot, A.N., and Jacobsen, S.B. (2013) ^{26}Al-^{26}Mg isotope systematics of the first solids in the early solar system. Meteoritics & Planetary Science, 48, 1383–1400.

Kööp, L., Nakashima, D., Heck, P.R., Kita, N.T., Tenner, T.J., Krot, A.N., Nagashima, K., Park, C., and Davis, A.M. (2016) New constraints for the relationship between ^{26}Al and oxygen, calcium, and titanium isotopic variation in the early Solar System from a multi-element isotopic study of Spinel-Hibonite Inclusions. Geochimica et Cosmochimica Acta, 184, 151–172.

Krot, A.N., Nagashima, K., Van Kooten, E.M.M., and Bizzarro, M. (2017a) High-temperature rims around calcium-aluminum-rich inclusions from the CR, CB and CH carbonaceous chondrites. Geochimica et Cosmochimica Acta, in press.

Krot, A.N., Nagashima, K., Van Kooten, E.M.M., and Bizzarro, M. (2017b) Calcium-aluminum-rich inclusions recycled during formation of porphyritic chondrules from CH carbonaceous chondrites. Geochimica et Cosmochimica Acta, in press.

Libourel, G., Krot, A.N., and Tissandier, L. (2006) Role of gas-melt interaction during chondrule formation. Earth and Planetary Science Letters, 251, 232–240.

Ma, C. (2015) Nanomineralogy of meteorites by advanced electron microscopy: Discovering new minerals and new materials from the early solar system. Microscopy and Microanalysis, 21 (Suppl 3), paper No. 1175 (Invited), 2353-2354.

Ma, C. and Krot, A.N. (2015) Addibischoffite, IMA 2015-006. CNMNC Newsletter No. 25, June 2015, page 532. Mineralogical Magazine, 79, 529–535.

Ma, C. and Rossman, G.R. (2008) Barioperovskite, $BaTiO_3$, a new mineral from the Benitoite Mine, California. American Mineralogist, 93, 154–157.

Ma, C. and Rossman, G.R. (2009) Tistarite, Ti_2O_3, a new refractory mineral from the Allende meteorite. American Mineralogist, 94, 841–844.

Ma, C., Beckett, J.R., and Rossman, G.R. (2010) Grossmanite, davisite, and kushiroite: Three newly-approved diopside-group clinopyroxenes in CAIs. 41st Lunar and Planetary Science Conference, Abstract #1494.

Ma, C., Kampf, A.R., Connolly, Jr H.C., Beckett, J.R., Rossman, G.R., Sweeney Smith, S.A., and Schrader, D.L. (2011) Krotite, $CaAl_2O_4$, a new refractory mineral from the NWA 1934 meteorite. American Mineralogist, 96, 709–715.

Ma, C., Krot, A.N., Beckett, J.R., Nagashima, K, and Tschauner, O. (2015) Discovery of warkite, $Ca_2Sc_6Al_6O_{20}$, a new Sc-rich ultra-refractory mineral in Murchison and Vigarano. Meteoritics and Planetary Science, 50 (S1), Abstract No. 5025.

Ma, C., Krot, A.N., and Nagashima, K. (2016a) Discovery of new mineral addibischoffite, $Ca_2Al_6Al_6O_{20}$, in a Ca-Al-rich refractory inclusion from the Acfer 214 CH3 meteorite. Meteoritics and Planetary Science, 51 (S1), Abstract No. 6016.

Ma, C., Paque, J., and Tschauner, O. (2016b) Discovery of beckettite, $Ca_2V_6Al_6O_{20}$, a new alteration mineral in a V-rich Ca-Al-rich inclusion from Allende. 47th Lunar and Planetary Science Conference, Abstract #1704.

McKeegan, K.D., Kallio, A.P.A., Heber, V.S., Jarzebinski, G., Mao, P.H., Coath, C.D., Kunihiro, T., Wiens, R.C., Nordholt, J.E., Moses, R.W.Jr., Reisenfeld, D.B., Jurewicz, A.J.G., and Burnett, D.S. (2011) The oxygen isotopic composition of the Sun inferred from captured solar wind. Science, 332, 1528−1532.

Tenner, T.J., Nakashima, D., Ushikubo, T., Kita, N.T., and Weisberg, M.K. (2015) Oxygen isotope ratios of FeO-poor chondrules in CR3 chondrites: Influence of dust enrichment and H_2O during chondrule formation. Geochimica et Cosmochimica Acta, 148, 228–250.

274 **Table 1**. Average elemental composition of six point EPMA analyses for type addibischoffite.

275

Constituent	wt%	Range	SD	Probe Standard
Al_2O_3	44.63	43.97–44.96	0.40	spinel
CaO	15.36	15.09–15.55	0.17	anorthite
SiO_2	14.62	14.44–15.07	0.23	anorthite
V_2O_3	10.64	9.77–11.12	0.48	V_2O_5
MgO	9.13	8.74–9.40	0.24	forsterite
Ti_2O_3	4.70	4.44–5.17	0.27	TiO_2
FeO	0.46	0.31–0.54	0.09	fayalite
Total	99.55			

276
277

278

279 **Table 2**. Oxygen-isotope compositions of individual minerals in the Acfer 214 CAI 1580-1-8.

mineral	$\delta^{18}O$	2σ	$\delta^{17}O$	2σ	$\Delta^{17}O$	2σ
hibonite	-37.4	1.5	-43.7	1.4	-24.3	1.6
addibischoffite	-38.7	1.9	-44.7	2.5	-24.6	2.7
Al-diopside	-9.4	1.9	-9.5	2.6	-4.6	2.8
Al-diopside	-6.7	1.9	-10.9	2.6	-7.4	2.8

280

This is a preprint, the final version is subject to change, of the American Mineralogist (MSA)
Cite as Authors (Year) Title. American Mineralogist, in press.
(DOI will not work until issue is live.) DOI: http://dx.doi.org/10.2138/am-2017-6032

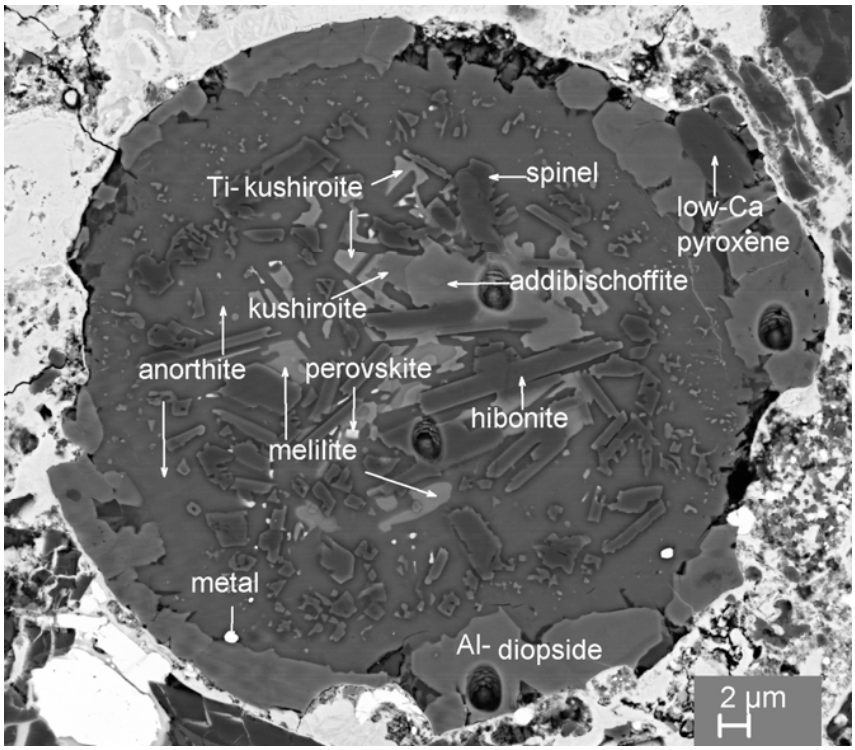

(a)

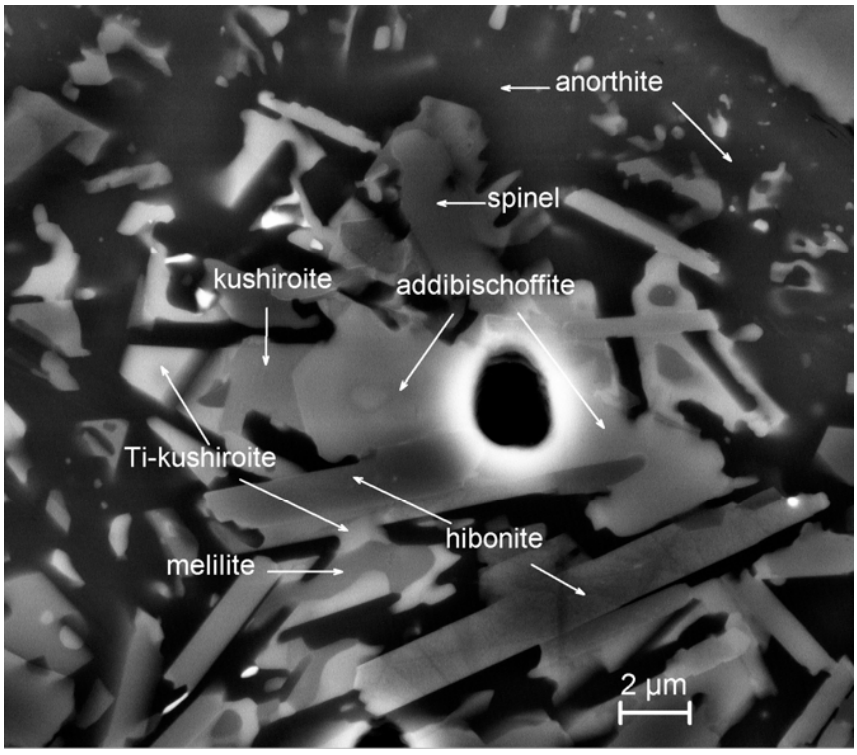

(b)

Figure 1. (a) Back-scatter electron (BSE) image showing addibischoffite in the CAI 1580-1-8 in section Acfer 214. The four holes in the CAI are ion probe pits. (b) Enlarged BSE image showing the type addibischoffite.

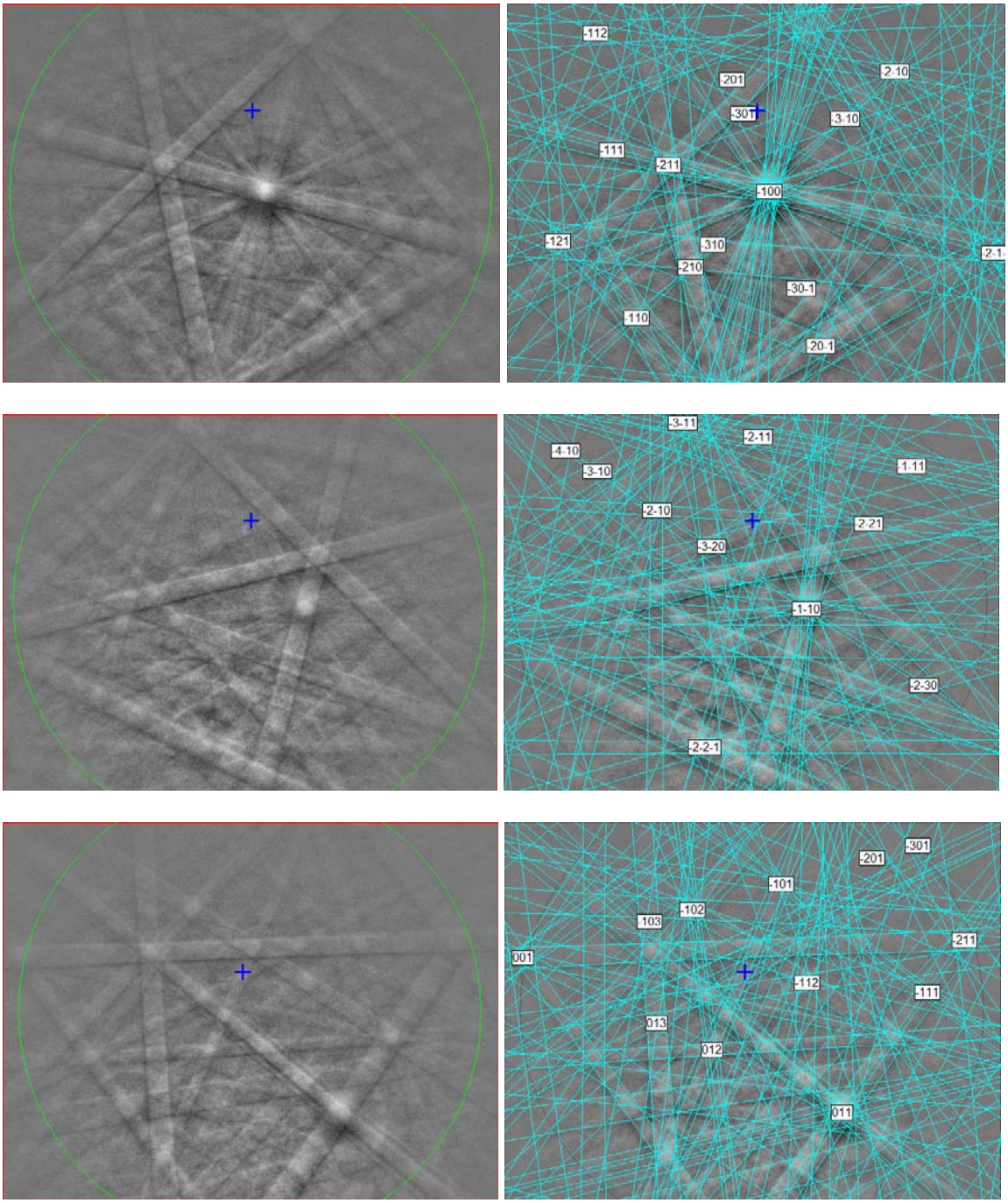

Figure 2. (left) EBSD patterns of the addibischoffite crystal in Fig. 1 at three different orientations, and (right) the patterns indexed with the $P\bar{1}$ rhönite structure.

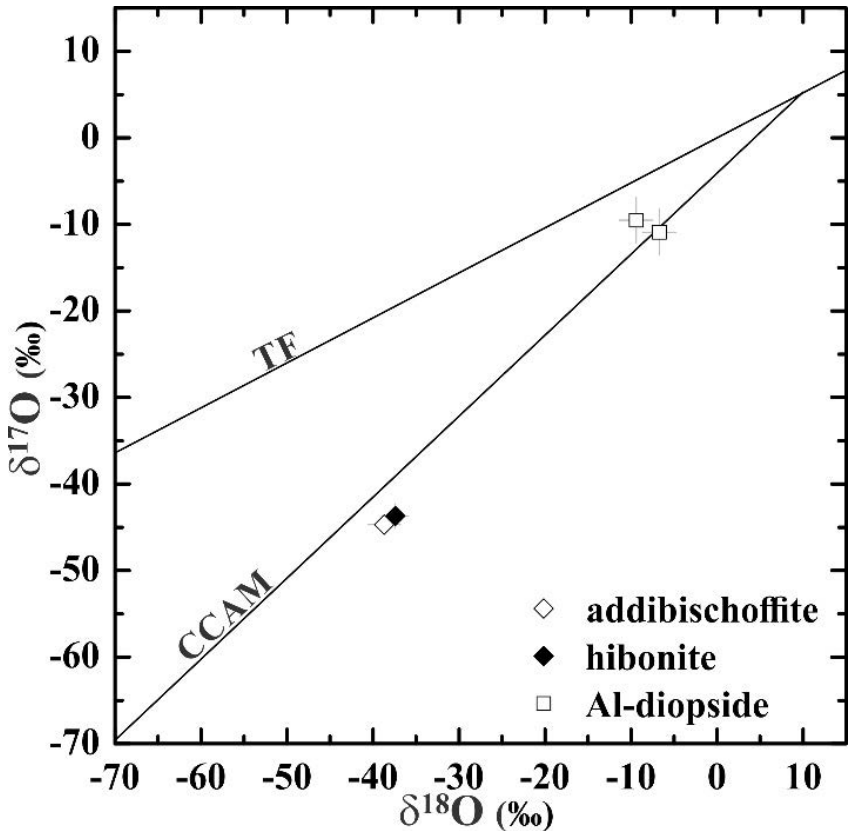

Figure 3. Three-isotope oxygen diagram showing compositions of addibischoffite, hibonite and Al-diopside in the Acfer 214 CAI 1580-1-8. The terrestrial fractionation (TF) line and carbonaceous chondrite anhydrous mineral (CCAM) line are shown for reference.